

Dear Natascha

So far, we have received 5 comments at dates: Aug. 20, Aug. 25, Sep. 25, Oct. 8 and Oct. 18 of 2014 and replied them during the next 12 days after the receptions. However, replying to your last e-mail about resending all the comments and replies in a new file, it will be send to you. In any case of duplicate or complementary comments and replies, it refers to the last reply. Meanwhile, figures **1, 2, 3, 7, 8 and 9** are edited based on reviewers' ordering.

20 August 2014

1-1) comments from Referees:

The novelty of this article is to propose to apply the well known Concentration area Multifractal classification model (Cheng et al., 1994) that was designed for extreme distribution detection on geochemical dataset, on the dataset on microtremor.

The Concentration Area classification model (C-A) is not fractal but multifractal (see Cheng et al., 1994). The text is often using fractal (supposed to be monofractal) and multifractal. Please clarify the text.

My main concern is about the use of C-A classification for more than two classes. The basic idea of C-A is to simplify asymptotically, the multifractal statistics in two scale domains: close to α_{\min} and close to α_{\max} . In both cases, the area statistics follow a scaling power law with different slope. This was done originally in order to separate usual variability and extreme fluctuation. The C-A model is not adapted for more than two classes. Cheng et al., 1994 discuss another type of model: the biofractal, which consist to claim that the geophysical data follow two monofractal scaling laws separated by a threshold scale. Both asymptotic multifractal and bifractal can create apparent break in the power law slopes.

1-1) Author's response:

Concentration-Area could be used for both monofractal and multimodal area. This method has been used for the booth and there are many references about it such as data characteristics have been determined even by multifractal method such as Afzal et al. (2010). Consequently, there is no need to change.

(Afzal, P., Khakzad, A., Moarefvand, P., Rashidnejad Omran, N., Esfan-diari, B., Fadakar Alghalandis, Y., 2010. Geochemical anomaly separation by multifractal modeling in Kahang porphyry system, Central Iran. Journal of Geochemical Exploration 104, 34–46)

1-2) comments from Referees:

Another comment is about the lack of justification of the classification on the frequency. Why the authors are choosing frequency (table 6) instead of amplification or k-g? Please justify this choice.

1-2) Author's response:

As it is mentioned in the paper we perform the C-A method to improve the Nogoshi's classification results in the Meybod city. This Classification and many other standard classifications are based on frequency or period. Additionally, it is said that the actual site amplification cannot be estimated from the amplitudes of HVSR peaks (Bard, 1998; Gosar et al., 2008; Sesame, 2004). Consequently, classification based on frequency is more reliable than amplification or k-g (as related to amplification).

1-3) comments from Referees:

Figure 2: “cultivated land” is not a geological unit but a vague pedological concept.

1-3) Author's response:

Please replace the new figure 2 instead of the earlier.

manuscript change

1-4) comments from Referees:

Figure 8 and figure 9: The comparison is hard between the two classification method.

Please plot all the microtremor points for both figures.

1-4) Author's response:

By adding microtremor points and names to the figure 8, the figure becomes very crowded and distinguishing the results may not be possible easily.

1-5) comments from Referees:

Please represent a classification map for figure 9, instead of an interpolated map.

1-5) Author's response:

The new figure 9 has been prepared and attached to the E-mail. Please replace it with the earlier.

manuscript change

25 August 2014

2-1) Comments from Referees:

Cheng and Agterberg (1996), Sim et al (1999), Goncalves et al (2001) are not using classification method for more than 3 classes but detection tool for extreme data (2 classes, as shown in all plots of those articles). The article from Afzal et al. (2010) proposes to extend the Concentration-Area method to more than two classes without theoretical justification. More than a theoretical work, this article should point out at least a discussion about the justification for the case of more than 2 classes, in the framework of fractal/multifractal. Also the authors should state clearly that their use of the C-A method is extended from the initial version from Cheng et al., 1994.

2-1) Author's response:

Cheng et al (1994) did not use any limitation for the C-A method entitled a bi-fractal method. They introduced the model for bi-fractal and multifractal natures (see section 4.1 and Appendix of the paper). They wrote formulation for both of them in this Appendix. Cheng and Li (2002) used the model in multifractal nature data. Many researchers used the method for multifractal modelling (e.g., as follow:(Cheng, Q., 1994, Multifractal modeling and spatial analysis with GIS: Gold potential estimation in the Mitchell-Sulphurets Area, Northwestern British Columbia: unpublished Ph. D. thesis, University of Ottawa, Ottawa, 268p.

Cheng, Q., 1997, Fractal/multifractal modeling and spatial analysis, in Proceedings of the International Association for Mathematical Geology Conference, V. Pawlowsky-Glahn (ed.), Barcelona, Spain, September 22-27, 1, 57-72.

Cheng, Q., 1999, Spatial and scaling modeling for geochemical anomaly separation. Journal Geochemical Exploration, 65 (3), 175-194.

Goncalves, M. A., Vairinho, M., and Oliveira, V., 1998, Study of geochemical anomalies in Mombeja area using a multifractal methodology and geostatistics, In Proceedings of International Association for Mathematical Geology Meeting. A. Buccianti, G. Nardi, and R. Potenza (eds.), De Frede, Ischia Island, Italy, 2. 590-595.

Goncalves, M.A., 2001. Characterization of geochemical distributions using multifractal models. *Math. Geol* 33 (1), 41-61.

Goncalves, M.A., Mateus, A., Oliveira, V., 2001. Geochemical anomaly separation by multifractal modeling. *Journal of Geochemical Exploration* 72, 91-114.

Cheng Q., Li Q., A fractal concentration-area method for assigning a color palette for image representation. *Computers & Geosciences.*, 2002, 28, 567-575

Lima, A., De Vivo, B., Cicchella, D., Cortini, M., Albanese, S., 2003. Multifractal IDW interpolation and fractal filtering method in environmental studies: an application on regional stream sediments of (Italy), Campania region, *Applied Geochemistry* 18, 1853–1865.

2-2) Comments from Referees:

Figure 3: the scale is still missing.

2-2) Author's response:

Please replace the new figure 3, the new figure has been attached.

manuscript change

2-3) Comments from Referees:

Figure 8: The points without names will improve the visibility of the figure and the comparison with figure 9.

2-3) Author's response:

The new figure has been attached.

manuscript change

2-4) Comments from Referees:

Figure 9: The figure would be more easy to interpret in color using the same color legend than figure 8.

2-4) Author's response:

The new figure 9 has been prepared and attached to the E-mail. Please replace it with the earlier.

manuscript change

25 September 2014

3-1) Comments from Referees:

Please find here an excerpt of Section 4.1 from Cheng et al., 1994: "In Appendix A it is shown in detail that if the element concentration per unit area satisfies a fractal or multifractal model, then the area $A(p)$ has indeed a power-law type relation with p . When the concentration per unit area follows a fractal model, this power-law relation has only one exponent. On the other hand, when the concentration per unit area satisfies a multifractal model with a spectrum of fractal dimensions, then several separate power-law relations between area $A(p)$ and p can be established. For a range of p close to its minimum value p the predicted multifractal power-law relations are: Equation (2a) where C_1 and C are constants

and α_1 and α_2 are exponents associated with the maximum singularity exponent. For a range of p close to its maximum value p_{max} , the predicted power law relation is: Equation (2b) where C_1 is another constant and C is the exponent associated with the minimum singularity exponent (see Appendix A)." The two extreme asymptotical relationships are developed for p close to minimum and maximum.

The appendix A contains the mathematical developments of those two asymptotical relationships, which is the heart of the article: separating geochemical "anomalies" from "background". All graphs presented in this article show one or two linear asymptotical domain in log/log space but never more than 2 linear domains. Again, several power laws can be established in the multifractal case, which apparently the case of your data but there is no rationale in the Concentration-Area model to identify them. A discussion of this point should appear in the article.

Cheng and Agterberg (1996), Sim et al (1999), Goncalves et al (2001) are not using classification method for more than 3 classes but detection tool for extreme data (2 classes, as shown in all plots of those articles).

The article from Afzal et al. (2010) proposes to extend the Concentration-Area method to more than two classes without theoretical justification. More than a theoretical work, this article should point out at least a discussion about the justification for the case of more than 2 classes, in the framework of fractal /multifractal. Also the authors should state clearly that their use of the C-A method is extended from the initial version from Cheng et al., 1994.

3-1) Author's response:

Cheng et al (1994) did not use any limitation for the C-A method entitled a bi-fractal method. They introduced the model for bi-fractal and multifractal natures (see section 4.1 and Appendix of the paper). They wrote formulation for both of them in this Appendix. Cheng and Li (2002) used the model in multifractal nature data. Many researchers used the method for multifractal modelling (e.g., as follow):

Cheng, Q., 1994, Multifractal modeling and spatial analysis with GIS: Gold potential estimation in the Mitchell-Sulphurets Area, Northwestern British Columbia: unpublished Ph. D. thesis, University of Ottawa, Ottawa, 268p.

Cheng, Q., 1997, Fractal/multifractal modeling and spatial analysis, in Proceedings of the International Association for Mathematical Geology Conference, V. Pawlowsky-Glahn (ed.), Barcelona, Spain, September 22-27, 1, 57-72.

Cheng, Q., 1999, Spatial and scaling modeling for geochemical anomaly separation. *Journal Geochemical Exploration*, 65 (3), 175-194. Goncalves, M. A., Vairinho, M., and Oliveira, V., 1998, Study of geochemical anomalies in Mombeja area using a multifractal methodology and geostatistics, In Proceedings of International Association for Mathematical Geology Meeting. A. Buccianti, G. Nardi, and R. Potenza (eds.), De Frede, Ischia Island, Italy, 2. 590-595. Goncalves, M.A., 2001. Characterization of geochemical distributions using multifractal models. *Math. Geol* 33 (1), 41-61. Goncalves, M.A., Mateus, A., Oliveira, V., 2001. Geochemical anomaly separation by multifractal modeling. *Journal of Geochemical Exploration* 72, 91-114. Cheng Q., Li Q., A fractal concentration-area method for assigning a color palette for image representation. *Computers & Geosciences.*, 2002, 28, 567-575 Lima, A., De Vivo, B., Cicchella, D., Cortini, M., Albanese, S., 2003. Multifractal IDW

interpolation and fractal filtering method in environmental studies: an application on regional stream sediments of (Italy), Campania region, Applied Geochemistry 18, 1853–1865.

manuscript change

8 October 2014

4-1) Comments from Referees:

The improvement of the figure, in particular the explicit values of the fits and the R² are significant. The rationale of the “linear-portion” are better demonstrated. Nevertheless, the text is still incomplete. The “linear-portion” in a log-log plot is not a signature of multifractal but it could also be a fractal by scale! Again the reference Agterberg et al., 1996 is never arguing on such “linear- portion”. In order to demonstrate the “multifractal” nature of their data, Agterberg et al., 1996 used different statistical moments. For each moment, a single power-law is demonstrated empirically (only one linear fit) but the exponent is different.

The reference Spalla et al. 2010 is new but not complete. Please add the full reference.

4-1) Author's response:

Based on the reviewer comment, We add descriptions about multifractal natures of my parameters in the area. Fig. 7 is edited and power-law relationships with R² are added to the log-log plots for showing of multifractal nature of the data.

There are multifractal natures for frequency, amplification and K-g based on the more than two straight segments. The straight segments fitted lines were derived based on least-square regression (Agterberg et al., 1996; Spalla et al., 2010). All R-squared values are higher than 0.9 and most of them have R² higher than 0.95 which is show a proper correlation (Fig. 7). The power-law relationships between the geophysical parameters and their occupied areas were indicated in the Fig. 7. According to the Eq. 2, there is different values for) which is exponent equal to fractal dimensions, as depicted in Fig. 7. The variation of fractal dimensions reveals a multifractal nature for frequency, amplification and K-g in the area.

manuscript change

18 October 2014

5-1) Comments from Referees:

Thank you for an interesting and valuable contribution that deserves publication.

Even so, I have a serious concern, reservation: based on the histogram of amplification's and k-g's values in the figure 4, is there really a justification for grouping all these data into one data set?

It seems rather obvious that there are likely to be multiple populations, presumably related to geology, e.g. lithology. Certainly from my point of view I would expect that anyone looking at this data would consider at least the relationship between lithology and multiple domains for different frequencies' populations? This should be discussed through the contents of the paper!

With respect to the Fig.5 of histograms, more statistical analysis should be conducted | however; the lack of adequate information is feeling!

According Fig.1, there are too many information on the Map of Iran which makes it overcrowded! The authors are highly recommended to replace this map with a readable one.

5-1) Author's response:

Thank you very much for your valuable comments. The answer of your questions and corrections are follow:

1. Frequency, amplification and k-g are different variables which reveal various characteristics of soils in the urban areas. The frequency and k-g show velocity of the wave and power of destruction. Combination of the three parameters cannot be possible. For more description for classical statistics the following sentences are added in lines 167-171:

The separated populations are clear in their histograms and also, high amounts of the parameters are lower than their means. Moreover, their median could be assumed for their threshold values because their distributions are not normal.

2. The microtremor data used for classification of different grounds of an urban area (may relates to different compaction or density and etc.) not just for lithological separation. The study area is located on a silty and clay plain (quaternary units), so we describe about soil types derived via the boreholes (Section 2). Based on the resulted frequencies, the most parts of the city contain soft soils. As it is mentioned in the Section 2, there is not any major variation in the composition of sediment in the area, except for some variation of clay and silt contents in the eastern part based on boreholes data. However, shear wave velocity data shows that there are differences in soil hardness values within the area. Consequently, one can concludes that the different category of frequency, amplification or k-g value may relate to variation of soil hardness in different places of the city.

3. Figure 1: The new figure has been attached, Please replace it with the earlier.

1 Site effect classification based on microtremor data 2 analysis using Concentration-area fractal model

3
4 **Ahmad Adib^{1*}, Peyman Afzal^{1,2}, Kobra Heydarzadeh³**

5 [1]{Department of Mining Engineering, Faculty of Engineering, South Tehran Branch, Islamic Azad
6 University, Tehran, Iran}

7 [2] {Camborne School of Mines, University of Exeter, Penryn, UK}

8 [3]{Zamin Kav Environmental & Geology Research Center, Tehran, Iran}

9 *Correspondence to: Ahmad Adib (adib@azad.ac.ir)

10 11 **Abstract**

12 The aim of this study is to classify the site effect using concentration-area (C-A) fractal model
13 in Meybod city, Central Iran, based on microtremor data analysis. Log-log plots of the
14 frequency, amplification and vulnerability index (k-g) indicate a multifractal nature for the
15 parameters in the area. The results obtained from the C-A fractal modeling reveal that proper
16 soil types are located around the central city. The results derived via the fractal modeling were
17 utilized to improve the Nogoshi's classification results in the Meybod city. The resulted
18 categories are: (1) hard soil and weak rock with frequency of 6.2 to 8 Hz, (2) stiff soil with
19 frequency of about 4.9 to 6.2 Hz, (3) moderately soft soil with the frequency of 2.4 to 4.9 Hz,
20 and (4) soft soil with the frequency lower than 2.4 Hz.

21 **Keywords:** Site effect classification, Concentration-area fractal model, Microtremor,
22 Frequency, Meybod city, Iran

23 24 **1 Introduction**

25 Site effect caused by an earthquake may vary significantly in a short distance. , Seismic
26 waves trapping phenomenon leads to amplify vibrations amplitudes that may increase hazards
27 in sites with soft soil or topographic undulations. Theoretical analysis and observational data
28 have illustrated that each site has a specific resonance frequency at which ground motion gets
29 amplified (Bard, 2000; Mukhopadhyay and Bormann, 2004).

1 Microtremor data analysis is applied in the recognition of the soil layers, prediction of shear-
2 wave velocity of the ground, and evaluation of the predominant period of the soil during
3 earthquake events. It has been proved that measurement and analysis of microtremor data is
4 an efficient and low-cost method of seismic hazard micro zonation (Kanai and Tanaka, 1954;
5 AIJ, 1993; Mukhopadhyay and Bormann, 2004; Beroya et al., 2009). Microtremors are weak
6 ground motions with amplitude between 1 and 10 μm which always exist and are mostly
7 generated by natural processes. Since these motions change the site effects and these changes
8 are representative of the soil characteristics, microtremors analysis is used to obtain
9 information about soil vibration properties of sites (Kamalian et al., 2008).

10 Some scientists believe that the microtremors are mostly formed by Love and Rayleigh waves
11 (Akamatu, 1961). However, they could be composed of Longitudinal and Rayleigh waves
12 (e.g. Douze et al., 1964). Allam (1969) proposed that microtremors could be composed of
13 body and/or surface waves and thus, it is possible that they are originated from any wave.

14 Microtremors are also applied to calculate the amplifications of horizontal movements in the
15 free surface during earthquake events (Nakamura, 1989). Fundamentally, the method
16 expressed the spectral amplification of a surface layer which could be obtained by evaluation
17 of the horizontal to vertical spectral ratio of recorded microtremors. The amplification factor
18 was resulted by several refracted waves in effect of their incidence into layer boundary. Thus,
19 associated Rayleigh wave of microtremor would be a noise and is removed during H/V
20 process. Moreover, H/V ratios of simultaneously measured records on ground surface and
21 bedrock represented constant maximum acceleration ratio. Since every station has different
22 characteristics, the records of one earthquake in various sites will be different. In soft soil
23 location underlying a hard rock, H/V spectral ratio illustrates a clear peak. These peaks are
24 spatially and temporally stable and could be considered as a fundamental (resonance)
25 frequency of the site (Duval et al., 1994; Duval, 1996). This method is used by many
26 scientists in order to identify small scale seismic risks and prepare detailed data for urban
27 seismic microzonation. Konno and Ohmachi (1998) carried out a complete study about
28 Nakamura's approximation and developed the matter to investigate multi-layered systems
29 which is known as HVSR method. It is obtained from numerical studies of horizontal
30 geological deposits that if there would be large impedance differences between deposits and
31 bedrock, local fundamental frequency could be well presented by HVSR method. However,
32 comparison of HVSR peaks with standard spectral ratio shows that the actual site

1 amplification cannot be estimated from the amplitudes of HVSR peaks (Bard, 1998; Gosar et
2 al., 2008; Sesame, 2004).

3 Identification of ground types is a main issue in the seismic geotechnical studies as well as
4 site selection. There are many site effect classifications based on dynamical ground
5 characteristics such as frequency, period, alluvial thickness, and shear wave velocity. Nogoshi
6 and Igarashi (1971) proposed one of the common classifications of site effects (Table 2).

7 Additionally, Komak Panah et al.(2002) presented a classification based on HVSR method in
8 the eastern and central Iran. Both used fundamental frequency as a main factor (Tables 1 and 2).

9
10 Euclidean geometry recognizes geometrical shapes with an integer dimension; 1D, 2D, and
11 3D. However, there are many other shapes or spatial objects whose dimensions cannot be
12 mathematically explained by integers, but by real numbers or fractions. These spatial objects
13 are called fractals. In abstract form, fractals describe complexity in data distribution by
14 estimation of their fractal dimensions. Different geophysical and geochemical processes can
15 be described based on differences in fractal dimensions obtained from analysis of relevant
16 geophysical data. Fractal models which established by Mandelbrot (1983) were applied to
17 objects that were too irregular to be described by ordinary Euclidean geometry (Davis, J.C.,
18 2002; Evertz and Mandelbrot, 1992). Fractal theory has been practical to geophysical and
19 geochemical exploration since late 1980s (e.g., Agterberg et al., 1996; Afzal et al., 2010;
20 2011; 2012; 2013; Cheng et al., 1994; Daneshvar et al., 2012; Sim et al., 1999; Turcotte,
21 1986). Cheng et al. (1994) proposed a concentration-area(C-A) fractal model based on the
22 relationship of elemental distributions and occupied areas. This idea and premise provided a
23 scientific tool to demonstrate that an empirical relationship between C-A exists in the
24 geophysical and geochemical data (Afzal et al., 2010; 2012; Cheng et al., 1994; Cheng, 1999;
25 Goncalves et al., 2001; Sim et al., 1999). Cheng et al. (1994) showed that there are various
26 parameters which have a key role in spatial distributions of most of the elements for a given
27 geological-geochemical environment.

28 In this paper, fundamental frequency, amplification and ground vulnerability index (K-g
29 value) data of Meybod city (Central Iran) are separated by C-A fractal model and Nogoshi's
30 classification. Subsequently, results obtained by the both methods are compared.

31

2 Case study characteristics

Meybod city is located in the Yazd province, central Iran (Fig 1), with Quaternary sediments as the major geological units (Fig. 2). Major types of the sediments are clay and ~~silty-silty-~~ clay in the area. Additionally, ~~Sandy-Sandy-~~clay units occurred in the ~~northeast-NE~~ part of the city with 2 m thickness and deep as 30-32 m.

Based on the geotechnical studies of the region, dominant soil type is composed of clay and silt with high plasticity (Fig 3). Additionally, there is not any major variation in the composition of sediment in the area, except for some variation of clay and silt contents in the eastern part (based on borehole data) (Fig 3).

From the downhole data which are collected from 5 boreholes, the variations of P and S velocity (m/s) were calculated (table 3). Shear wave velocity is between 560 and 725 m/s in the depth of 42 m. the depth of seismic bedrock varies ~~from 52~~ from 52 to 90 m which are calculated based on the velocity. This result shows that there are differences in soil hardness values within the area.

3 Methodology

Measured microtremor data were analyzed by Nakamura technique (HVSR: Nakamura, 1989) and using SESAME software, based on Fast Fourier Transform (FFT). The results were mapped by Inverse Distance Squared (IDS) method using Rockworks TM v.15 software package. The results are fundamental frequency, amplification and ground vulnerability index (K-g value); K-g value has obtained by Equation (1): (Nakamura, 1996):

$$Kg = (A_0)^2 / F_0 \quad (1)$$

where F_0 and A_0 are predominant frequency and its amplification factor, and K-g is an index to indicate deformation easiness of measured points which is expected to be useful to detect weak points of the ground (Nakamura, 1997).

For instance, K-g values obtained in San Francisco Bay Area after the 1989 Loma-Prieta Earthquake are bigger than 20 at the sites where grounds were deformed significantly and very small at the sites with no damage (Nakamura et al., 1990). However, ~~comparison~~ Comparison between K-g values obtained before the earthquake in 1994 and the damage

1 degrees show that places with large K-g values correspond to the sites with big damage. This
2 suggests K-g values representing the vulnerability precisely (Nakamura, 1997).

3 **3.1 Concentration–area fractal model**

4 Cheng et al. (1994) proposed concentration–area (C–A) model, which may be used to define
5 the geophysical background and anomalies. The model is in the following general form:

$$6 \quad A(\rho \leq \nu) \propto \rho^{-a_1}; A(\rho \geq \nu) \propto \rho^{-a_2} \quad (2)$$

7 where $A(\rho)$ is the area with concentration values (frequency, amplification and K-g in this
8 study) greater than the contour value ρ ; ν is the threshold; and a_1 and a_2 are characteristic
9 exponents.

10 The frequency size distributions for islands, earthquakes, fragments, ore deposits and oil
11 fields often confirm the Equation (2) (Daneshvar Saein et al., 2012). The two approaches
12 which were used to calculate $A(\rho)$ by Cheng et al. (1994) were: (1) The $A(\rho)$ is the area
13 enclosed by contour level ρ on a variables' contour map resulting from interpolation of the
14 original data using a weighted moving average method, and (2) The $A(\rho)$ are the values that
15 are obtained by box-counting of original regional variables' values. The breaks between
16 straight-line segments on C-A log-log plot and the corresponding values of ρ have been used
17 as thresholds to separate geophysical values into various components, showing different
18 causal factors, such as lithological and mineralogical differences, geochemical and
19 geophysical processes and mineralizing events (Lima et al., 2003; Afzal et al., 2010; 2012;
20 Heidari et al., 2013).

21 Fractal models are often used to describe self-similar geometries, while multifractal models
22 have been utilized to quantify patterns; same as geophysical data defined on sets which
23 themselves can be fractals. Extension from geometry to field has considerably increased the
24 applicability of fractal/multifractal modeling (Cheng, 2007). Multifractal theory could be
25 interpreted as a theoretical framework that explains the power-law relationships between areas
26 enclosing concentrations below a given threshold value and the actual concentrations itself.
27 To demonstrate and prove that data distribution has a multifractal nature requires a rather
28 extensive computation (Halsey et al., 1986; Evertsz and Mandelbrot, 1992). This method has
29 several limitations such as accuracy problems, especially when the boundary effects on
30 irregular geometrical data sets are involved (Agterberg et al., 1996; Goncalves, 2001; Cheng,
31 2007; Xie et al., 2010).

1 The C-A model seems to be equally applicable as well to all cases, which is probably rooted
2 in the fact that geophysical distributions mostly satisfy the properties of a multifractal
3 function. Some evidence prove that geophysical data distributions are fractal in nature and
4 behavior (e.g., Bolviken et al., 1992, Turcotte, 1997, Gettings, 2005, Afzal et al., 2012, and
5 Daneshvar Saein et al. 2012).

6 This idea may provide and help the development of an alternative interpretation validation as
7 well as useful methods to be applied to geophysical distributions analysis (Afzal, 2012).
8 Various log-log plots between a geometrical character such as area, perimeter or volume and a
9 geophysical quality parameter ~~like~~ such as geoelectrical data in fractal methods are
10 appropriate for distinguishing geological recognition and populations' classification in
11 geophysical data because threshold values can be identified and delineated as breakpoints in
12 those plots (Daneshvar Saein et al., 2012).

13

14 **4 Application of C-A model**

15 Microtremor data are measured at 160 point in the study area (Fig. 1) using three channeled
16 seismometer device (SL07, SARA Company, Italy). It has natural frequency of 2 Hz and
17 natural attenuation of 0.7. This device has a three channeled digitizer of 24 bit, a central
18 process unit (CPU) to save records and a GPS receiver. The data were recorded by sampling
19 frequency of 200 Hz and the average recording time of 12 minutes at each station. At first, a
20 mesh was overlapped on the city map to determine the recording points. Then, recording on
21 every point was regularly performed. When any of recording points was not appropriate for
22 recording (e.g. because of existence of tall buildings), the point location was slightly shifted
23 to achieve a clear data. Moreover, if any point was approximate to a heavy traffic street, the
24 data were recorded at midnight. During recording process, the device was located on a leveled
25 ground and was balanced. Usually, 10 min is required for any microtremor recording to
26 record the minimum 1 Hz frequency (WP12 Sesame project, 2004).

27 The obtained frequencies, amplifications and K-g values are illustrated as contour maps
28 applying IDS interpolation method (Fig. 4). The areas with different frequencies can be
29 visually distinguished in the map. The studied area was gridded by 20×20 m cells. The
30 evaluated values in cells were sorted out based on decreasing grades, and cumulative areas
31 were calculated for grades. Eventually, log-log graphs were plotted to separate the different
32 populations.

1 Distributions of the fundamental frequency, amplification and K-g data are multimodal which
2 their mean values are 3.24 Hz, 2.14 and 2.91, respectively (Fig. 5). The separated populations
3 are clear in their histograms and also, high amounts of the parameters are lower than their
4 means. Moreover, their median could be assumed for their threshold values because their
5 distributions are not normal—. The medians are 2.6 Hz, 1.6 and 1.1 for frequency,
6 amplification and K-g respectively. Moreover, the median values of these parameters are low
7 for their threshold values. Variograms and anisotropic ellipsoids of the parameters were
8 calculated to estimate data influence range of any point in order of plotting IDS maps (Fig. 6).
9 These ellipsoids make the results estimated more accurate and we can determine the direction
10 of the results variations. Based on the variograms and ellipsoids of the parameters, their major
11 ranges have a W-E trend. It could be represented by the direction of soil variations that
12 become more intense from west to the east of the area (Fig. 3).

13
14 According to the C-A log-log plots, four populations were distinguished for the frequency and
15 five populations for the amplification and K-g which reveals multifractal nature for the
16 parameters in the Meybod city, as depicted in Fig 7. There are multifractal nature for
17 frequency, amplification and K-g based on the more than two straight segments. The straight
18 segments fitted lines were derived based on least-square regression (Spalla et al., 2010). All
19 R-squared values are higher than 0.9 and most of them have R^2 higher than 0.95 which is
20 show a proper straight line fitting for the populations(Fig. 7). The power-law relationships
21 between the geophysical parameters and their occupied areas were indicated in the Fig. 7.
22 According to the Eq. 2, there is different values for α which is exponent equal to fractal
23 dimensions, as depicted in Fig. 7. The variation of fractal dimensions reveals a multifractal
24 nature for frequency, amplification and K-g in the area. Moreover, a sudden exchanges shows
25 different populations in the log-log plots which (Fig. 5). Data distribution based on C-A
26 model has been shown in Fig 8. The sites with high intensity values of frequency are situated
27 in the central parts of the area and the sites with high intensive amplification and K-g are
28 located in the northern and eastern parts of the Meybod city.

29 The most part of the city has frequency lower than 4.9 Hz, especially between 2.4 to 4.9 Hz.
30 The central part of the city is the only part with high frequency, as depicted in Fig 8. It
31 represents that it is more competent than the other parts. Based on the resulted frequencies,
32 the most parts of the city contain soft soils, but amplification and K-g quantities are very low,
33 lower than 2.4 and 4.2, respectively.

1

2 **5 Comparison between Nogoshi classification and Fractal modeling results**

3 Site classification of the city is calculated based on Nogoshi and Igarashi method (1970;
4 1971) which is a common classification for microtremor analysis. The basis of this
5 classification is fundamental frequency, thus, with regard to the obtained frequencies, ground
6 type of Meybod is achieved that it has shown in Table 3 and Fig 9.

7

8 Comparison between the C-A fractal model and Nogoshi classification shows that the
9 thresholds obtained by the both methods are similar (Table 4). Indeed it can be said that by
10 frequency separation resulted from fractal C-A model, we can identify data minor anomalies
11 and consequently classify site effect results more accurately. Therefore, by this approach
12 other results due to frequency, can be classified and then every category attributed to one
13 specific ground type.

14 By comparing the soil zonation maps, it is obvious that there are five categories for
15 amplification and K-g value. Meanwhile, there are four categories due to frequency and
16 ground classification. Generally, the amplification of the city is low because of very low
17 variation in the soil composition. Based on the amplification and K-g values (Table 5) of
18 every frequency category, appropriate quantities of amplification and vulnerability index in
19 any resulted classes of the C-A fractal model were derived (Table 6). Accordingly,
20 amplification and k-g in any frequency category are respectively: lower than 2.7 and lower
21 than 1.2 for frequency between 6.2-8 ~~Hz~~, lower than 5.4 and lower than 4.2 for frequency
22 4.9-6.2 and lower than or equal to 10 and 40 for the other both frequency groups.

23

24 Based on the results obtained by shear wave velocity calculation in the boreholes and results
25 derived via the C-A fractal model, the velocities were correlated with threshold values of the
26 C-A model (Table 3).

27

28 **6 Conclusions**

29 The C-A fractal model is a useful approach in geophysical analysis to identify anomalies and
30 geological particulars and this has been proved by numerous studies. Also this method could
31 be appropriate for geophysical distribution analysis due to its fractal nature.

1 In this study, due to comparing site effect classification of the area based on Nogoshi and
2 Igarashi classification and frequency categorization resulted from the C-A fractal model, it is
3 obtained that the C-A fractal model is a useful tool to distinguish and classify site effect
4 results, so that category boundaries could be recognized more accurately. Therefore, the
5 results are presented better and more suitable and also we can attribute resulted frequency,
6 amplification and vulnerability index to any site class more confidently. Additionally, the
7 thresholds derived via Nogoshi and Igarashi classification for the region were corrected.
8 Accordingly, four site classes were obtained for the city as follows:

9 - Category 1 (weak rock, hard soil): Frequency between 6.2-8 Hz, amplification lower than
10 2.7 and vulnerability index lower than 1.2. It exists in some points of the center of the city
11 toward the east.

12 - Category 2 (stiff soil): Frequency between 4.9-6.2 Hz, amplification lower than 5.4 and
13 vulnerability index lower than 4.2. It exists mostly in the central parts of the city.

14 - Category 3 (moderately soft soil): Frequency between 2.4-4.9 Hz, amplification lower than
15 10 and vulnerability index lower than or equal to 40. It exists in the most parts of the city.

16 - Category 4 (soft soil): Frequency lower than 2.4 Hz, amplification lower than 10 and
17 vulnerability index lower than or equal to 40, similar to category 3. It is scattered in the
18 different parts of the city such as east and SE, west and SW, center and NW of the area.

19

20 **Acknowledgementsome**

21 The authors thank Islamic Azad University -South Tehran branch for support of this research.
22 In addition, the authors acknowledge Dr. Gholamreza shoei (assistant professor at
23 engineering geology group, geology section, Tarbiat Modares University) and Mr. Alireza
24 Ashofteh for their remarkable contribution.

25

26 **References**

27 Afzal, P., Zia Zarifi, A., Yasrebi, A. B., 2012. Identification of uranium targets based on
28 airborne radiometric data analysis by using multifractal modeling, Tark and Avanligh
29 1:50000 sheets, NW Iran. Journal of Nonlinear Processes in Geophysics, 19, 283-289.

- 1 Afzal, P., Khakzad, A., Moarefvand, P., Rashidnejad Omran, N., Esfan-diari, B., Fadakar
2 Alghalandis, Y., 2010. Geochemical anomaly separation by multifractal modeling in Kahang
3 (Gor Gor) porphyry system, Central Iran. *Journal of Geochemical Exploration* 104, 34–46.
- 4 Agterberg, F.P., Cheng, Q., Brown, A., Good, D., 1996. Multifractal modeling of fractures in
5 the Lac du Bonnet batholith, Manitoba. *Comput. Geosci.* 22 (5), 497–507.
- 6 Akamatu, K., 1961. On microseisms in frequency range from 1 c/s to 200 c/s. *Bull.*
7 *Earthquake Res. Inst.*, 39: 23-75.
- 8 Allam, A. M., 1969. An Investigation Into the Nature of Microtremors Through Experimental
9 Studies of Seismic Waves. University of Tokyo, 326 p.
- 10 Architectural Institute of Japan, 1993. Earthquake Motion and Ground Condition. AIJ, AIJ, 5-
11 26-20 Shiba, Minato-ku, Tokyo 108, *Japan*
- 12 Bard, P. Y., 1998. Microtremor measurements: a tool for site effects estimation? Proceedings
13 of the Second International Symposium on the effects of Surface Geology on Seismic Motion,
14 Yokohama, Japan, December 1998, 1251–1279, 1998TS5.
- 15 Bard, P.Y., 2000. Lecture notes on ‘Seismology, Seismic Hazard Assessment and Risk
16 Mitigation’. International Training Course, Potsdam, p. 160
- 17 Beroya, M.A.A., Aydin, A., Tiglao, R., Lasala, M., 2009. Use of microtremor in liquefaction
18 hazard mapping. *Engineering Geology* 107, 140-153.
- 19 Bolviken, B., Stokke, P.R., Feder, J., Jossang, T., 1992. The fractal nature of geochemical
20 landscapes. *J. Geochem. Explor.* 43, 91–109.
- 21 Cheng, Q., Agterberg, F.P., Ballantyne, S.B., 1994. The separation of geochemical anomalies
22 from background by fractal methods. *J. Geochem. Explor.* 51, 109–130.
- 23 Cheng, Q., 1999. Spatial and scaling modelling for geochemical anomaly separation. *J.*
24 *Geochem. Explor.* 65 (3), 175–194.
- 25 Cheng, Q., 2007. Mapping singularities with stream sediment geochemical data for prediction
26 of undiscovered mineral deposits in Gejiu, Yunnan Province, China. *Ore Geol. Rev.* 32, 314–
27 324.
- 28 Daneshvar Saein, L., Rasa, I., Rashidnejad Omran, N., Moarefvand, P., and P. Afzal, 2012.
29 Application of concentration-volume fractal method in induced polarization and resistivity

1 data interpretation for Cu-Mo porphyry deposits exploration, case study: Nowchun Cu-Mo
2 deposit, SE Iran. *Nonlinear Processes in Geophysics.*, 19, 431–438.

3 Davis, J.C., 2002. *Statistics and data analysis in Geology* (3th ed.). John Wiley & Sons Inc.,
4 New York, p. 638.

5 Douze E.J., 1964. Rayleigh waves in short period seismic noise. *Bull. Seism. Soc. Am.*, Vol.
6 54, 1197-1212.

7 Duval, A.M., 1994. Détermination de la réponse d'un site aux séismes à l'aide du bruit de
8 fond: Évaluation expérimentale. PhD Thesis. Université Pierre et Marie Curie, Paris 6. in
9 French.

10 Duval, A. M., 1996. Détermination de la réponse d'un site aux séismes à l'aide du bruit de
11 fond, Evaluation expérimentale, Etudes et Recherches des Laboratoires des Ponts et
12 Chaussées, Série Géotechnique. ISSN 1157-39106, 264 pp., Paris : Laboratoire central des
13 ponts et chaussées, ISBN 2-7208-2480 -1, in French, 264 pp.

14 Evertz, C.J.G., Mandelbrot, B.B., 1992. Multifractal measures (appendix B). In: Peitgen, H.-
15 O., Jurgens, H., Saupe, D. (Eds.). *Chaos and Fractals*, Springer, New York, p. 953.

16 Gettings, M.E., 2005. Multifractal magnetic susceptibility distribution models of
17 hydrothermally altered rocks in the Needle Creek Igneous Center of the Absaroka Mountains,
18 Wyoming. *Nonlinear Processes in Geophysics* 12, 587-601.

19 Goncalves, M.A., 2001. Characterization of geochemical distributions using multifractal
20 models. *Math. Geol* 33 (1), 41-61.

21 Goncalves, M.A., Mateus, A., Oliveira, V., 2001. Geochemical anomaly separation by
22 multifractal modeling. *J. Geochem. Explor.* 72, 91–114.

23 Gosar, A., Stoper, R., Roser, J., 2008. Comparative test of active and passive multichannel
24 analysis of surface waves (MASW) methods and microtremor HVSR method. *RMZMaterial*
25 *and Geo-environment* 55 (1), 41–66.

26 Gosar, A., Roser, J., 2010. Microtremor study of site effects and soil-structure resonance in
27 the city of Ljubljana (central Slovenia). *Bulletin of Earthquake Engineering* 8, 571–592.

28 Guest, B., Axen, G. J., Lam, P. S. and Hassanzadeh, J., 2006. Late Cenozoic shortening in the
29 west-central Alborz Mountains, northern Iran. *Geosphere*, 2, 35-52.

- 1 Halsey, T.C., Jensen, M.H., Kadanoff, L.P., Procaccia, I., Shraiman, B.I., 1986. Fractal
2 measures and their singularities: the characterization of strange sets. *Phys. Rev. A* 33 (2),
3 1141–1151.
- 4 Heidari, S.M., Ghaderi, M. and Afzal, P., 2013. Delineating mineralized phases based on
5 lithogeochemical data using multifractal model in Touzlar epithermal Au-Ag (Cu) deposit,
6 NW Iran. *Applied Geochemistry* 31, 119-132.
- 7 Kamalian, M., Jafari, M.K., Ghayamghamian, M.R., Shafiee, A., Hamzehloo, H.,
8 Haghshenas, E., Sohrabi-bidar, A., 2008. Site effect microzonation of Qom, Iran. *Engineering*
9 *Geology* 97, 63-79
- 10 Kanai, K., Tanaka, T., 1954. Measurement of the microtremor I. *Bulletin of the Earthquake*
11 *Research Institute* 32, 199-209.
- 12 Komak Panah, A., Hafezi Moghaddas, N., Ghayamghamian, M. R., Motosaka, M., Jafari, M.
13 K., and Uromieh, A., 2002. Site Effect Classification in East-Central of Iran. *Journal of*
14 *Seismology and Earthquake Engineering*, Vol.4, No.1, pp. 37-46,
- 15 Konno, K and Ohmachi, T., 1998. ground motion characteristics estimated from spectral ratio
16 between horizontal and vertical components of microtremor. *Bulletin of the Seismological*
17 *Society of America*, 88, 228–241.
- 18 Lima, A., De Vivo, B., Cicchella, D., Cortini, M., Albanese, S., 2003. Multifractal IDW
19 interpolation and fractal filtering method in environmental studies: an application on regional
20 stream sediments of (Italy), Campania region. *Applied Geochemistry* 18, 1853–1865.
- 21 Mandelbrot, B.B., 1983. *The Fractal Geometry of Nature*. W. H. Freeman, San Fransisco, p.
22 468.
- 23 Mukhopadhyay, S., Bormann, P., 2004. Low cost seismic microzonation using microtremor
24 data: an example from Delhi, India. *Journal of Asian Earth Sciences* 24, 271-280.
- 25 Nakamura, Y., 1989. A method for dynamic characteristics estimation of subsurface using
26 microtremor on the ground surface, *Quarterly report of Railway Technical Res. Inst. (RTRI)*,
27 30:1, 25-33.
- 28 Nakamura, Y., 1996. Real-time information systems for hazard mitigation. *Proceedings of the*
29 *10th World Conference in Earthquake Engineering*, Anchorage, Alaska, Paper # 2134.

- 1 Nogoshi, M. and T. Igarashi, 1971. On the amplitude characteristics of microtremor (Part 2).
2 Jour. seism. Soc. Japan, 24, 26-40 (in Japanese with English abstract).
- 3 Nogoshi, M. and T. Igarashi, 1970. On the propagation characteristics of microtremors.
4 Journal of the Seismological Society of Japan 23, 264-280.
- 5 SESAME, European research project WP12: 2004. Guidelines for the implementation of
6 the H/V spectral ratio technique on ambient vibrations: measurements, processing and
7 interpretation. Available at: http://sesame-fp5.obs.ujf-grenoble.fr/Delivrables/Del-D23-HV_User_Guidelines.pdf.
8 Last accessed July 2011.
- 9 Sim, B.L., Agterberg, F.P., Beaudry, C., 1999. Determining the cutoff between background
10 and relative base metal contamination levels using multifractal methods. Comput. Geosci. 25,
11 1023–1041.
- 12 [Spalla, M.I., Morotta, A.M., Gosso, G., 2010. Advances in interpretation of geological](#)
13 [processes: refinement of multi-scale data and integration in numerical modelling. Geological](#)
14 [Society, London, 240 p.](#)
- 15 Turcotte, D.L., 1986. A fractal approach to the relationship between ore grade and tonnage.
16 Econ. Geol. 18, 1525–1532.
- 17 Turcotte, D.L., 1997. Fractals and Chaos in Geology and Geophysics. Cambridge University
18 Press, Cambridge.
- 19 [Xie, S., Cheng, Q., Zhang, S., Huang, K., 2010. Assessing microstructures of pyrrhotites in](#)
20 [basalts by multifractal analysis. Nonlinear Processes in Geophysics 17, 319-327.](#)
- 21 **Table and Figures Caption lists:**
- 22 **Tables:**
- 23 [Table 1. Site effect classification of Komak Panah et al. \(2002\)](#)
- 24 [Table 2. Site effect classification of Nogoshi & Igarashi \(1970\)](#)
- 25 [Table 3. Velocity of seismic waves \(m/s\) in the Meybod city](#)
- 26 [Table 4. Comparison of frequency separation by C-A fractal model and Nogoshi & Igarashi](#)
27 [\(1970, 1971\).](#)
- 28 [Table 5. Frequency of amplification and K-g classes in every frequency category](#)

1 Table 6. Site effect classification based on C-A method

2 **Figures:**

3 Figure 1. Figure 1. A) The location of the study area (black star) in Iran; B) The microtremor
4 recording points and boreholes map.

5 Figure 2. Geological map of Meybod area. According to the map, the major units around the
6 city are Quaternary deposits including cultivated land, Clay flat and young terraces and fans.
7 The only other unit that is close to the city is Eocene gypsiferous Marls (Egm).

8 Figure 3. 3D model of soil deposits of Meybod city, Iran. Dominant soil type is composed of
9 clay and silt with high plasticity. The major variation is located in the eastern part of the city
10 (CL: inorganic Clay of low plasticity or lean Clay; MH: inorganic Silt of high plasticity; CL-
11 ML: inorganic Clay and inorganic Silt of low plasticity; CH: inorganic Clay of high plasticity;
12 ML: inorganic Silt of low plasticity; SM: silty Sand).

13 Figure 4. Data distribution maps in the Meybod city: A) frequency; B) amplification; C) K-g
14 value.

15 Figure 5. Data histograms show multimodality of the factors. A) Frequency, B) amplification,
16 C) K-g value

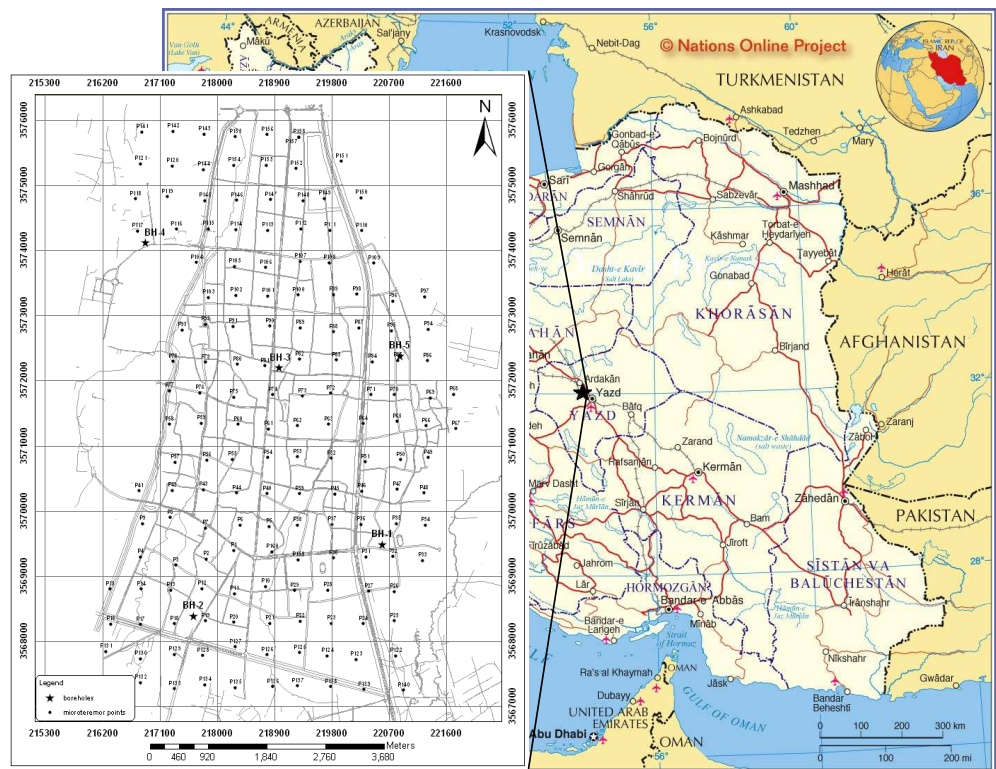
17 Figure 6. Variograms and anisotropic ellipsoids of the parameters: A) Frequency; B)
18 amplification; C) K-g value.

19 Figure 7. C-A log-log plot for the parameters: A) frequency, B) amplification, C) K-g value.

20 Figure 8. Data classification based on C-A method. A) frequency, B) amplification, C) K-g
21 value.

22 Figure 9. Ground type zonation of the region based on Nogoshi & Igarashi (1970, 71).

23

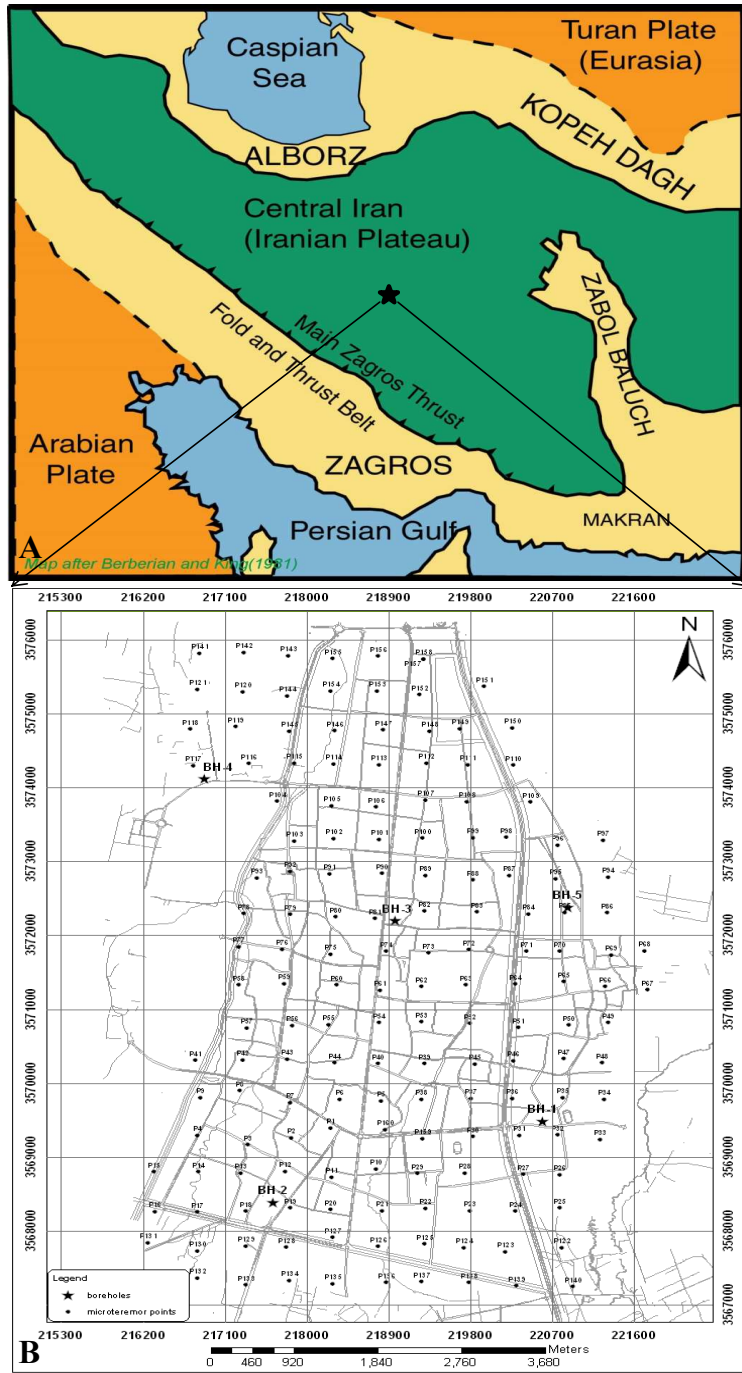


1
2
3
4
5
6
7
8
9
10
11
12
13

Figure 1. The political map of Iran (the Nations Online Project, 2014); the location of the study area (shown by a black star), and the microtremor recording points and boreholes map.

Figure change

1
2
3
4
5
6
7
8
9
10
11
12
13
14
15
16
17
18
19
20
21
22
23
24

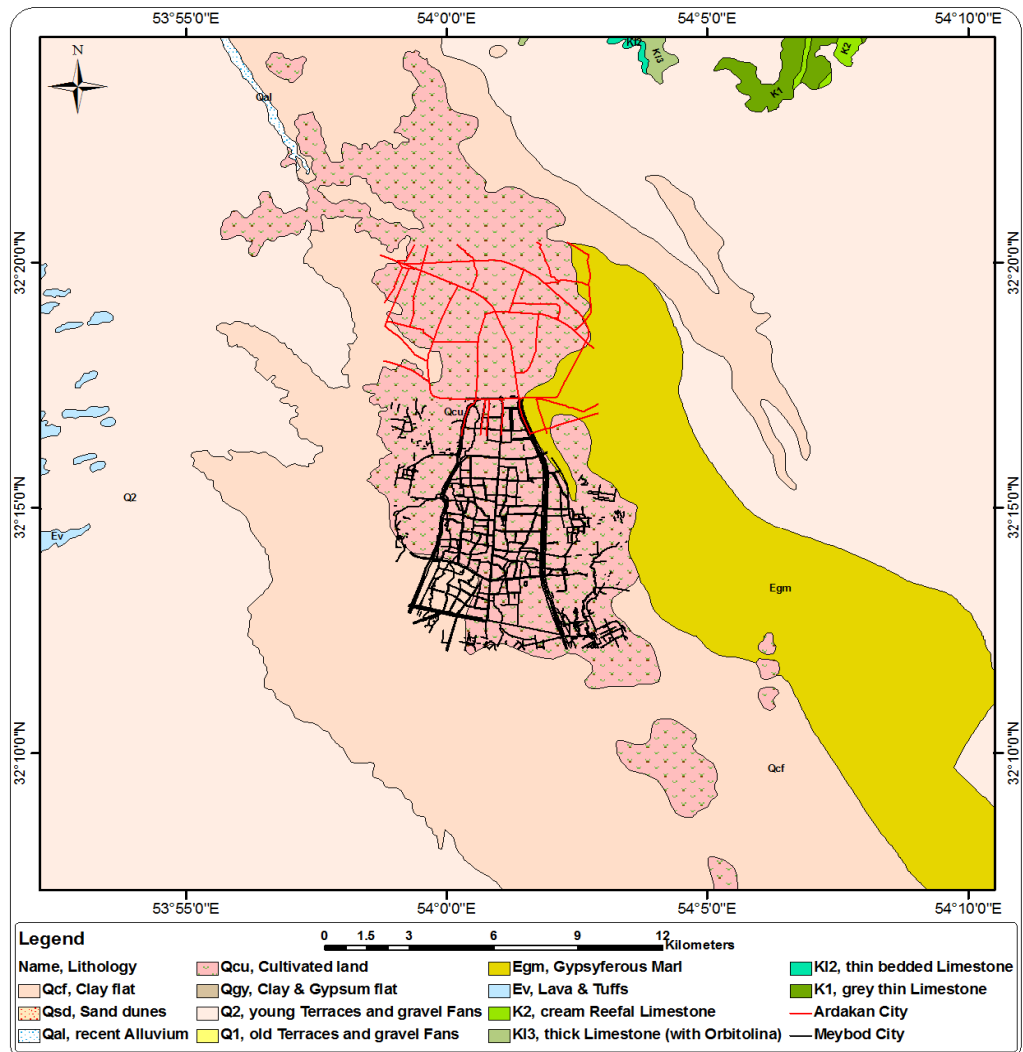


Formatted: Figure, Justified, Space Before: 6 pt, Line spacing: 1.5 lines

25 **Figure 1. A) The location of the study area (black star) in Iran; B) The microtremor recording points and boreholes map.**

26

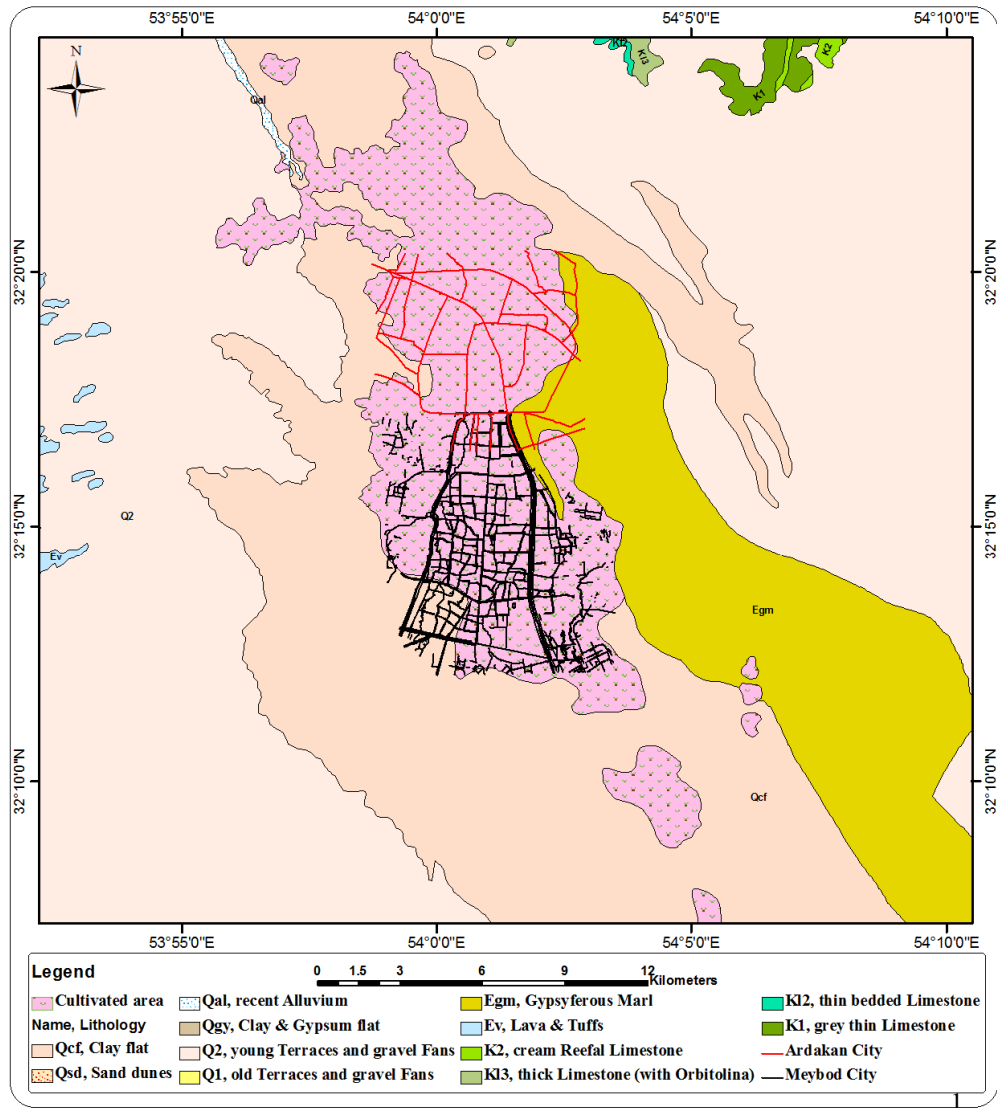
1
2
3
4



5
6
7
8
9

Figure 2. Geological map around Meybod city. According to the map, the major units around the city are Quaternary deposits including cultivated land, Clay flat and young terraces and fans. The only other unit that is close to the city is Eocene gypsiferous Marls (Egm).

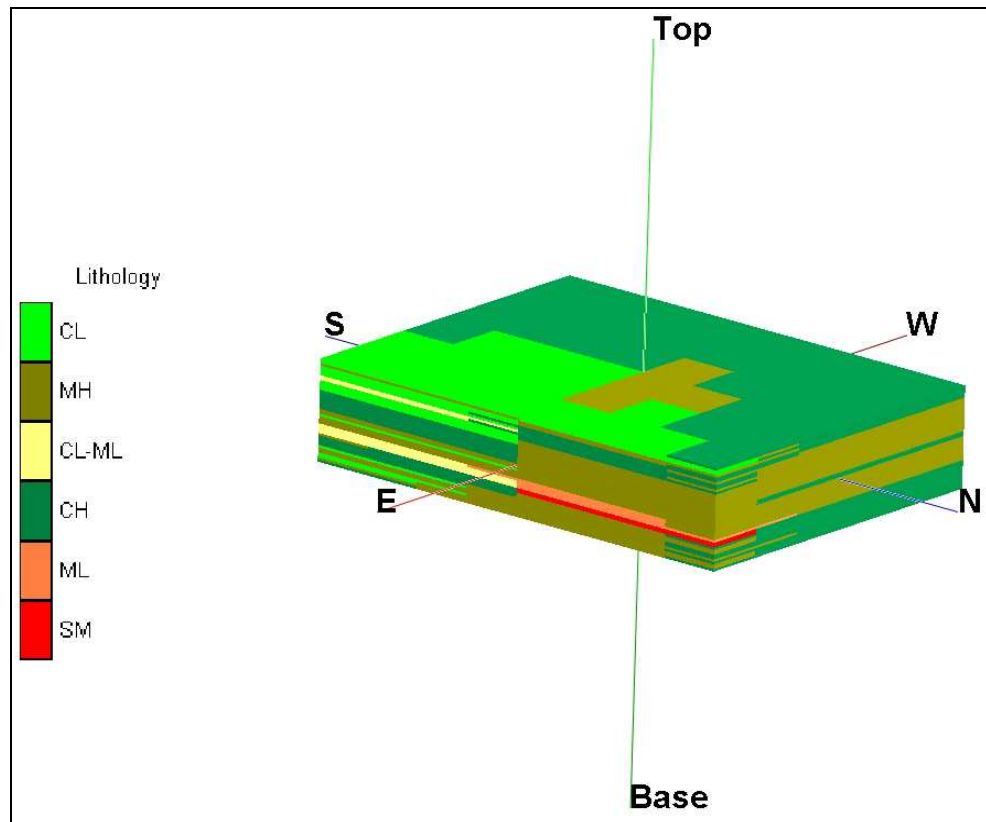
[Figure change](#)



Formatted: Justified

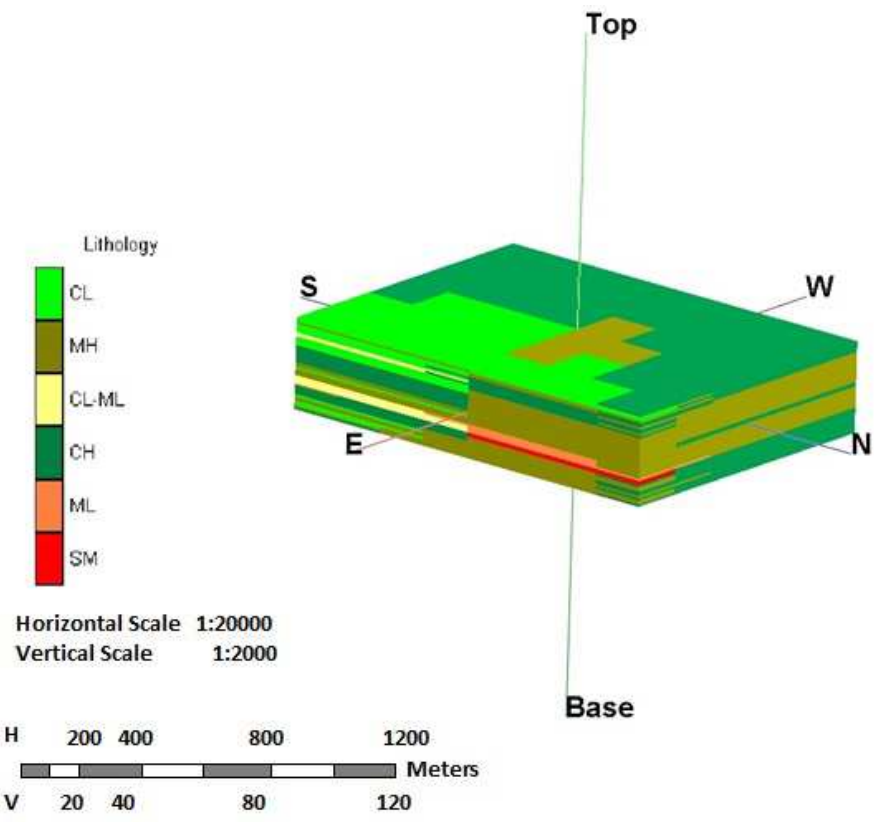
2 -> **Figure 2. Geological map of Meybod area. According to the map, the major units around the city are**
 3 **Quaternary deposits including cultivated land, Clay flat and young terraces and fans. The only other unit that is**
 4 **close to the city is Eocene gypsiferous Marls (Egm).**

5
6



1
2
3
4
5
6
7
8

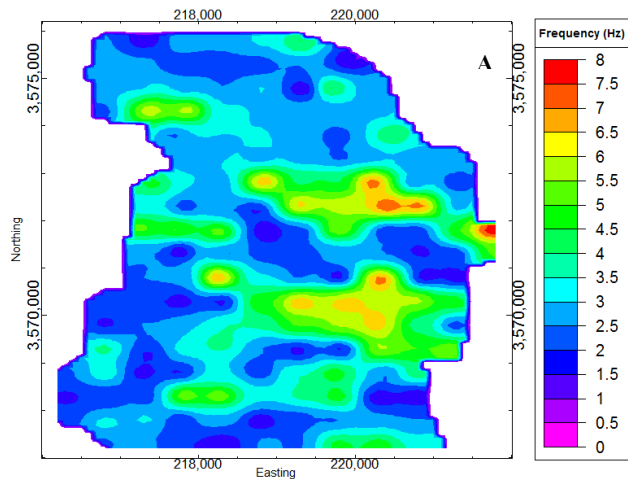
Figure 3. 3D model of soil deposits of Meybod city, Iran. Dominant soil type is composed of clay and silt with high plasticity. The major variation is located in the eastern part of the city (CL: inorganic Clay of low plasticity or lean Clay; MH: inorganic Silt of high plasticity; CL-ML: inorganic Clay and inorganic Silt of low plasticity; CH: inorganic Clay of high plasticity; ML: inorganic Silt of low plasticity; SM: silty Sand). [Figure change](#)



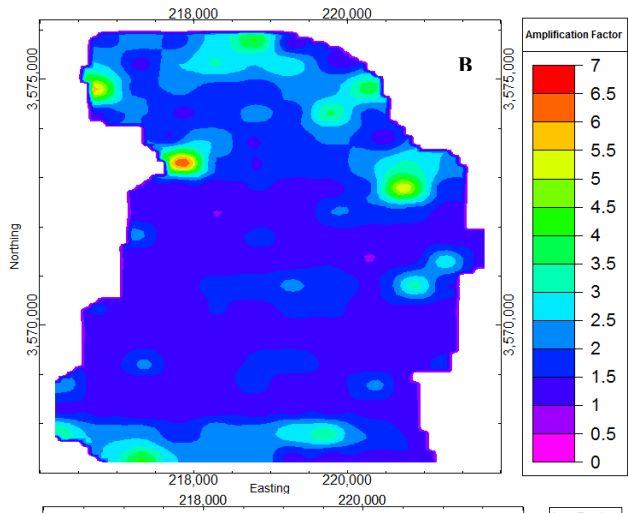
1

Formatted: Figure, Justified, Space Before: 6 pt, Line spacing: 1.5 lines

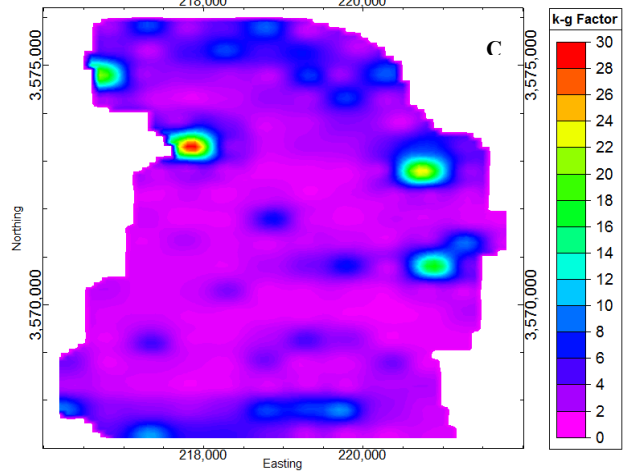
2 Figure 3. 3D model of soil deposits of Meybod city, Iran. Dominant soil type is composed of
 3 clay and silt with high plasticity. The major variation is located in the eastern part of the city
 4 (CL: inorganic Clay of low plasticity or lean Clay; MH: inorganic Silt of high plasticity; CL-
 5 ML: inorganic Clay and inorganic Silt of low plasticity; CH: inorganic Clay of high plasticity;
 6 ML: inorganic Silt of low plasticity; SM: silty Sand).



1

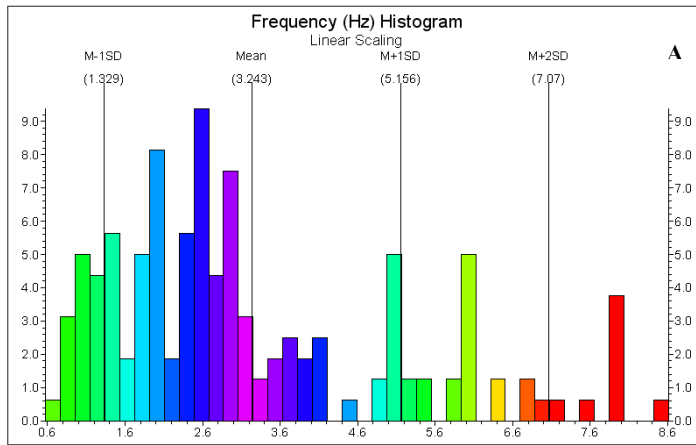


2

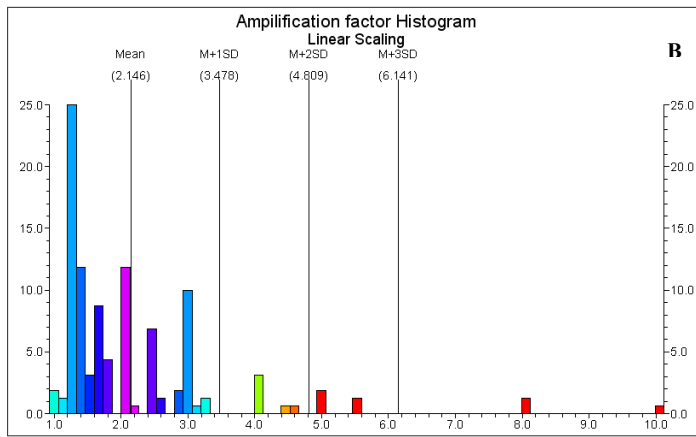


3

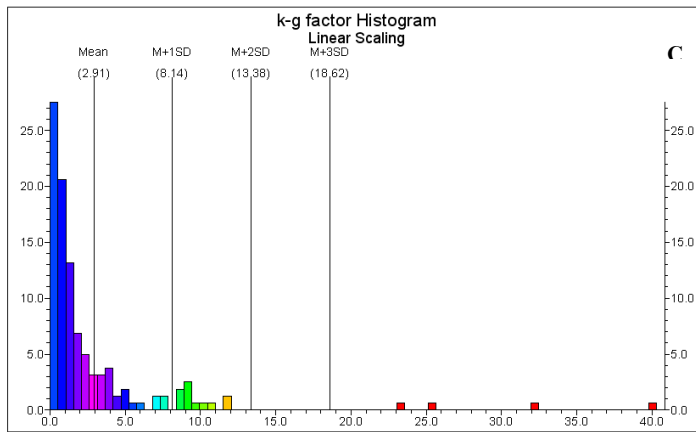
4 **Figure** Fig. 4. Data distribution maps in the Meybod city: A) frequency; B) amplification; C) K-g value.



1



2

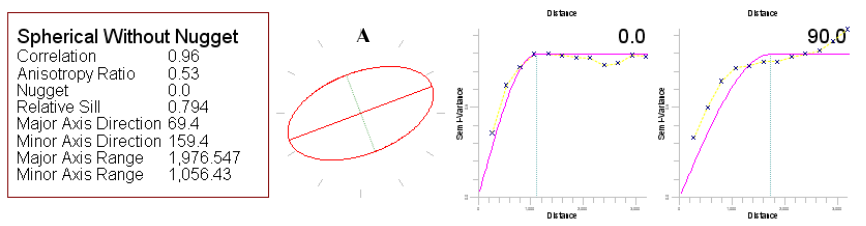


3

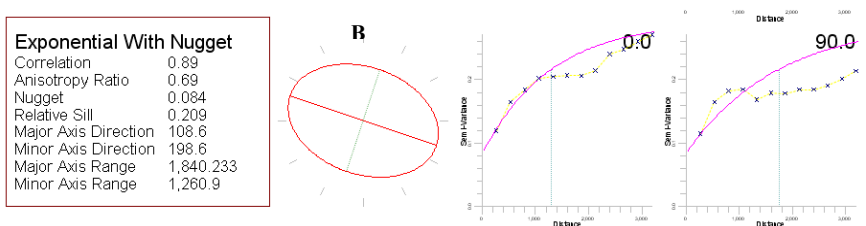
4 Figure 5. Data histograms show multimodality of the factors. A) Frequency, B) amplification,
5 C) K-g value

Formatted: English (United States)

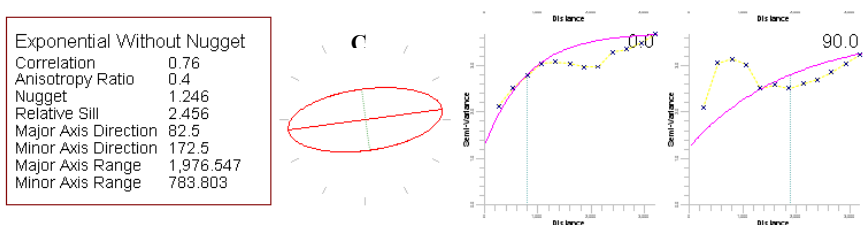
1



2



3



4

5 Figure 6. Variograms and anisotropic ellipsoids of the parameters: A) Frequency; B)
6 amplification; C) K-g value.

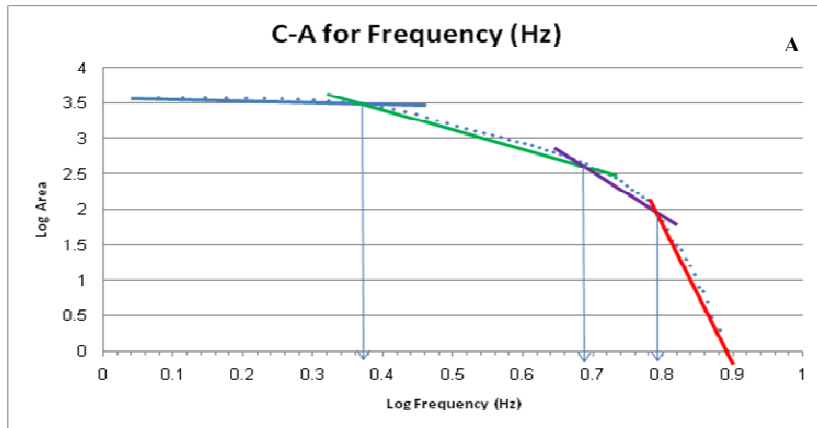
7

8

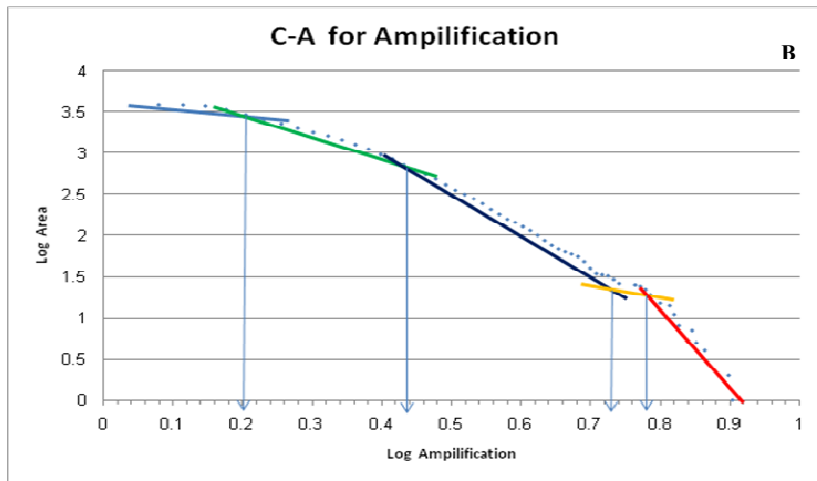
9

Formatted: English (United States)

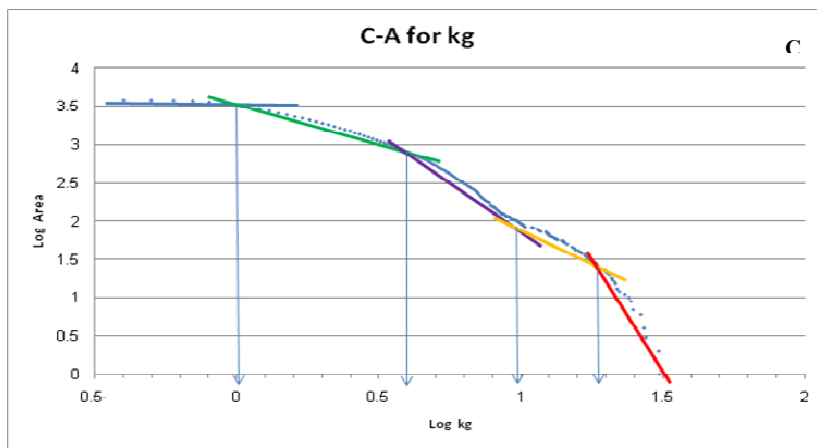
10



1



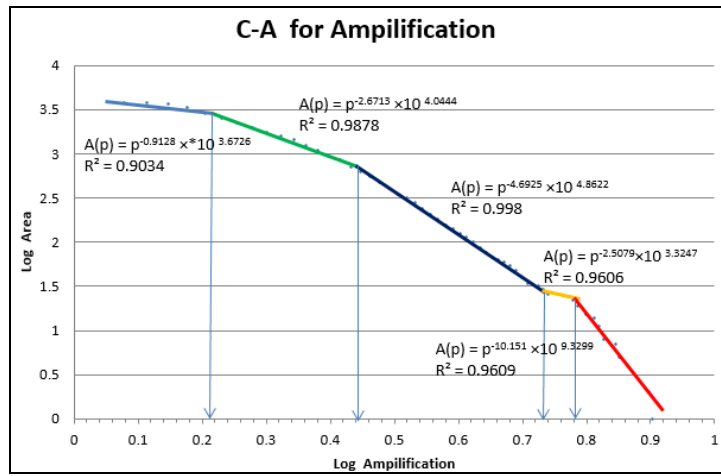
2



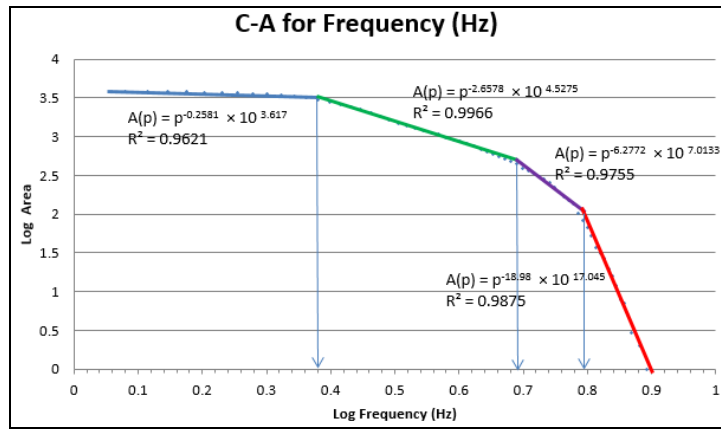
3

4 Figure 7. C-A log-log plot for the parameters: A) frequency, B) amplification, C) K-g value.

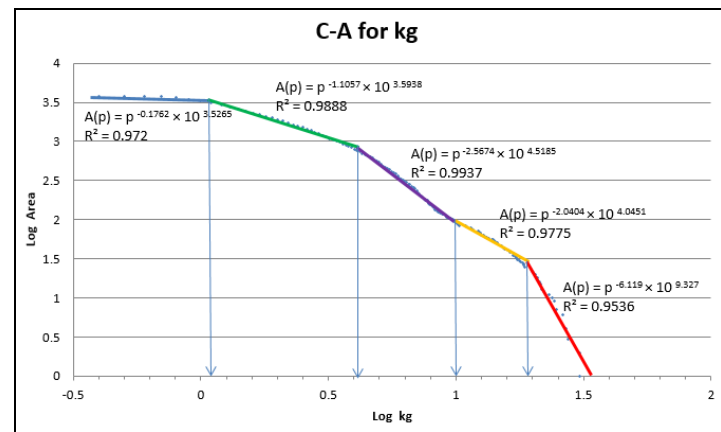
5 [Figure change](#)



1



2



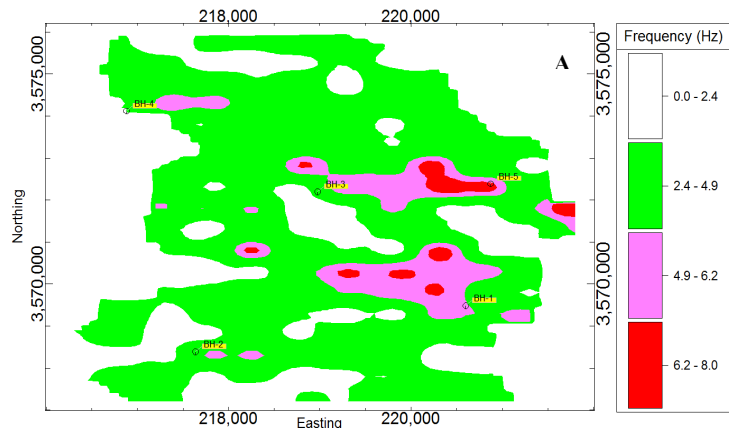
3

4

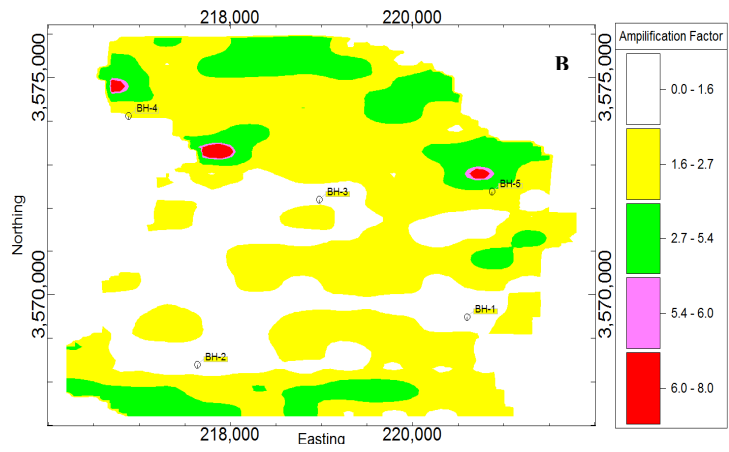
Figure 7. C-A log-log plot for the parameters: A) frequency, B) amplification, C) K-g value.

Formatted: English (United States)

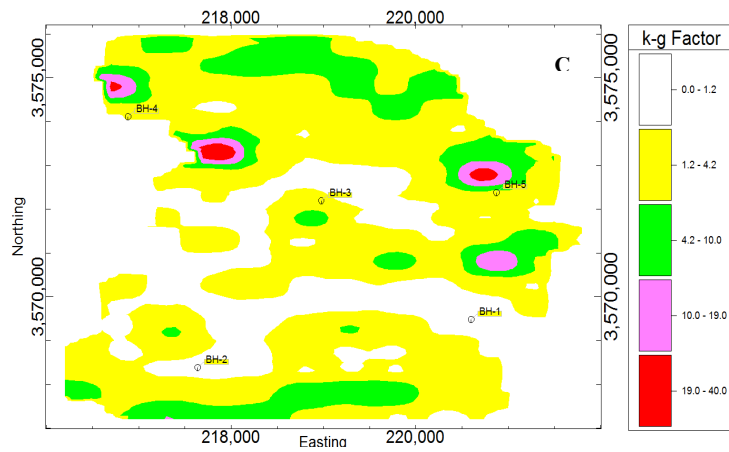
5



1



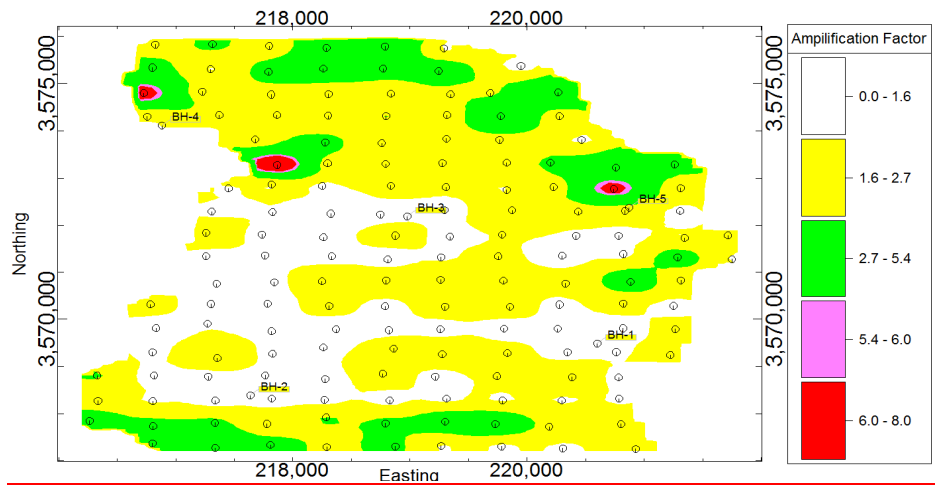
2



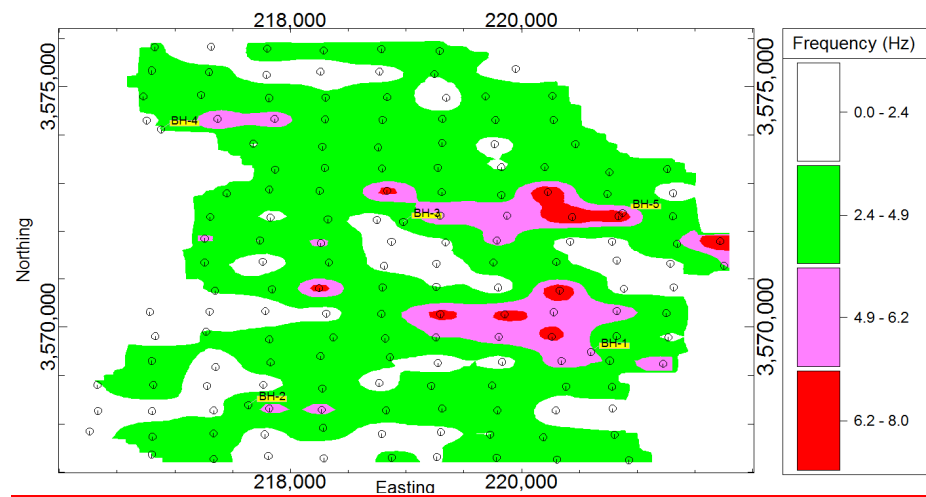
3

4 **FigureFig.** 8. Data classification based on C-A method. A) frequency, B) amplification, C)
 5 K-g value. Figur change

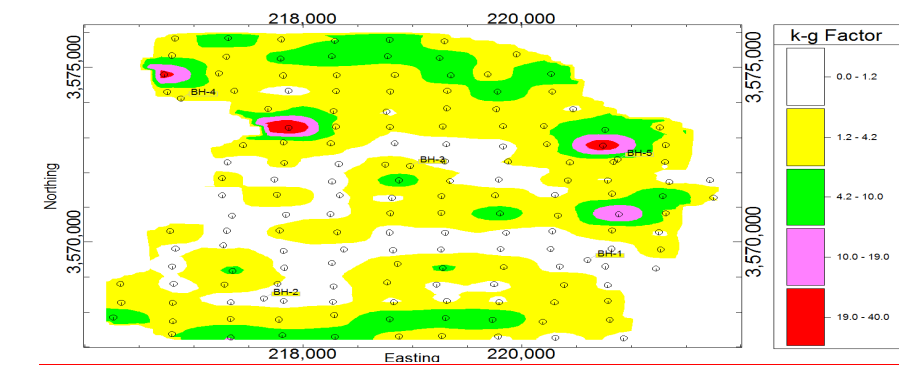
C



1



2

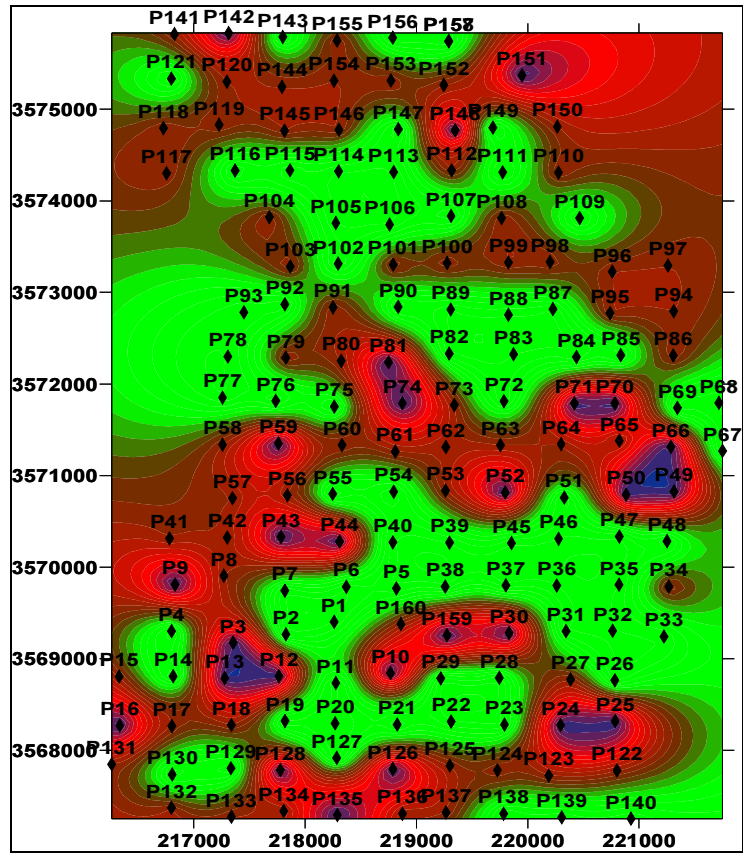


3

4 **Figure 8. Data classification based on C-A method. A) frequency, B) amplification, C) K-g**
 5 **value.**

C

1



2

3 Figure 9. Ground type zonation of the region based on Nogoshi & Igarashi (1970, 71). Violet
4 color (points 12, 13, 24, 25, 49, 50, 74 and 151) is ground type 4; (dark) red color represents
5 type 3 and (light) green color is type 2. [Figure change](#)

6

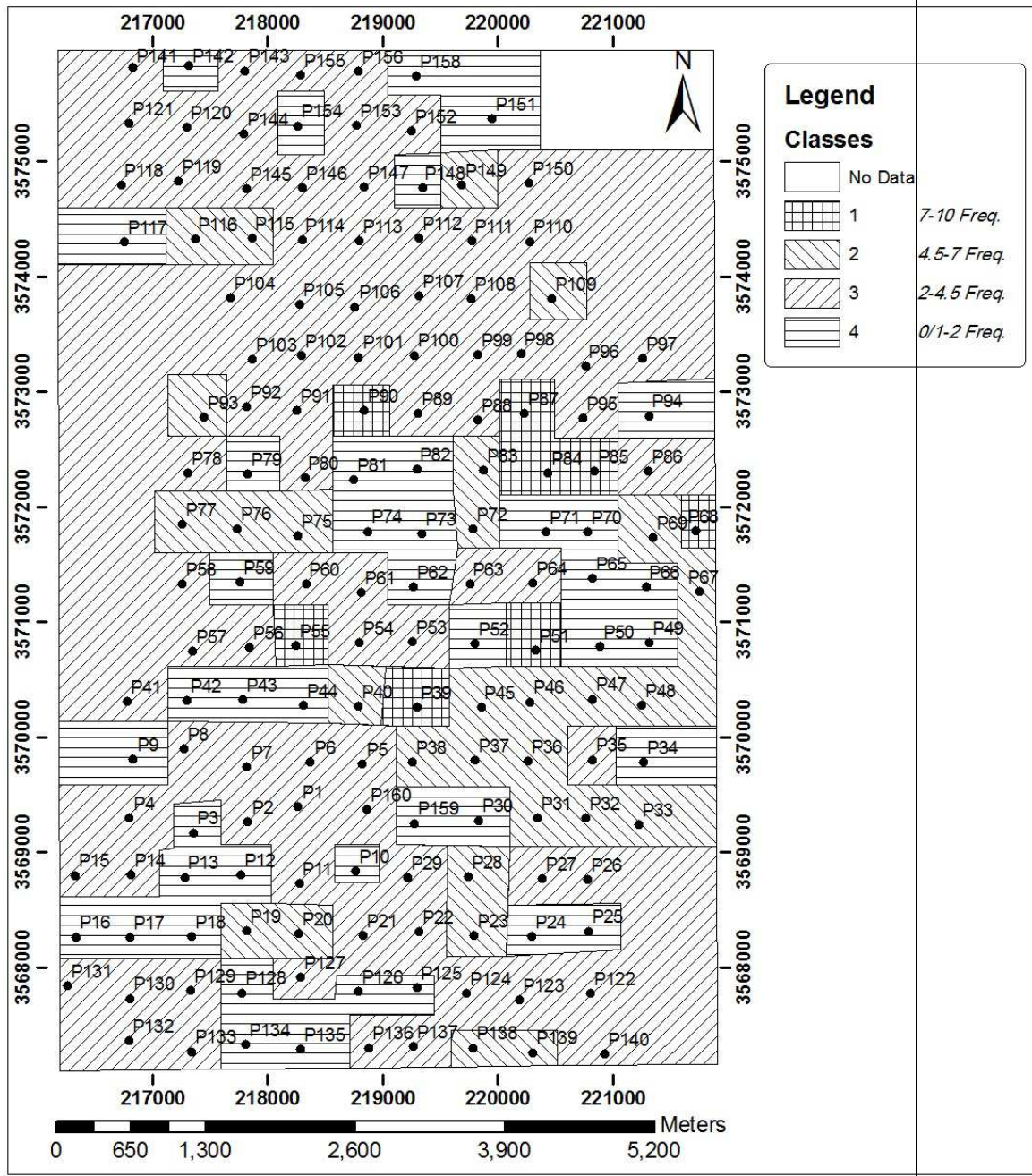
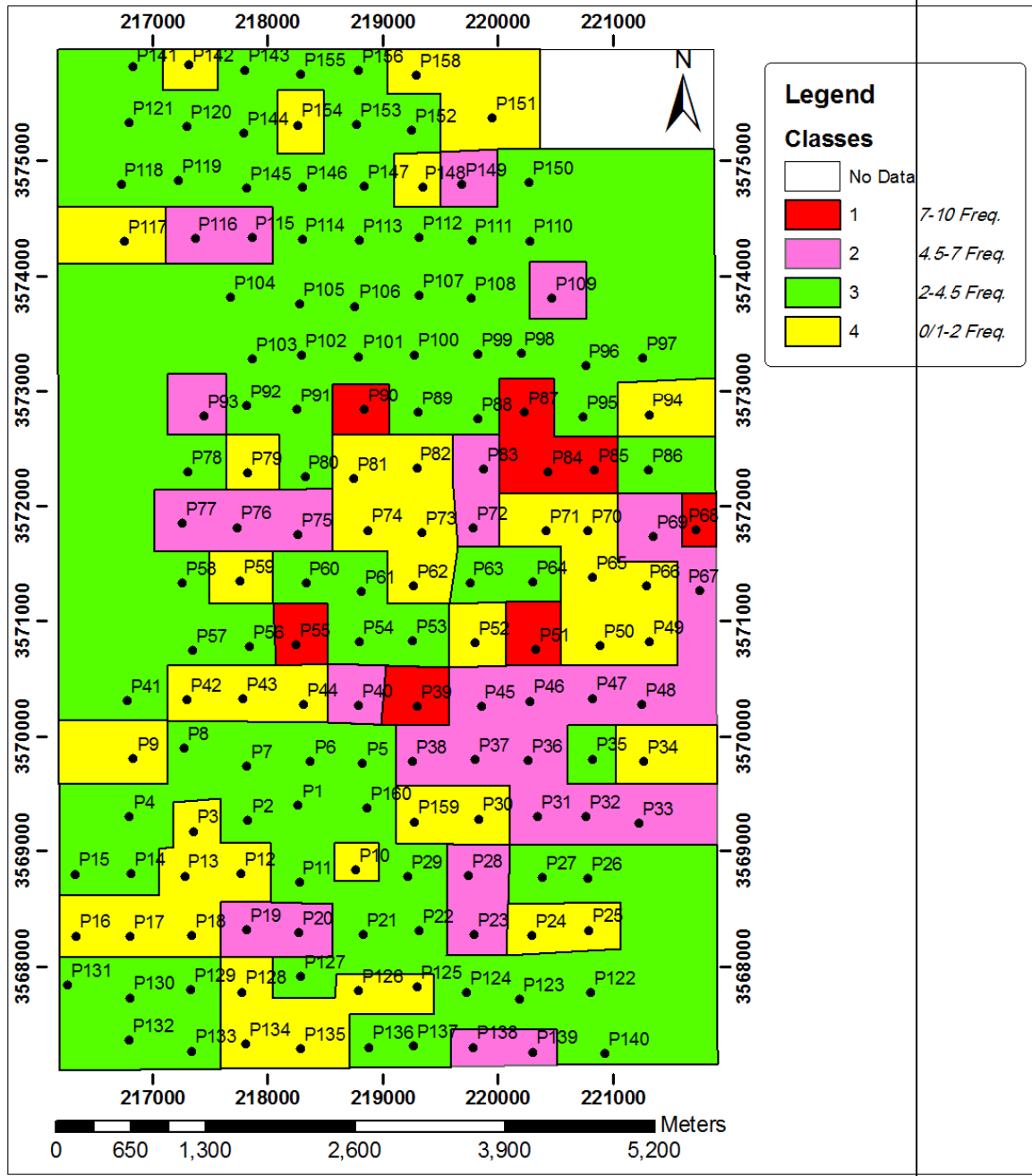


Figure.9. Ground type zonation of the region based on Nogoshi & Igarashi (1970, 71). Figure change

Formatted: Normal, Right, Space Before: 0 pt, Line spacing: single



1
2

Figure 9. Ground type zonation of the region based on Nogoshi & Igarashi (1970, 71).

Formatted: Normal, Centered, Space Before: 0 pt, Line spacing: single

3